

ORIGINAL RESEARCH

Open Access

Numerical and experimental analyses of an integral bridge

Yasser Khodair^{1*} and Sophia Hassiotis²

Abstract

In this paper, we present the analysis of a numerical and an experimental study of the Scotch Road integral abutment bridge located in Trenton, NJ, USA. Three-dimensional, nonlinear finite element (FE) model of the full bridge has been developed to study the effect of thermal loading on the bridge substructure. The bridge substructure was fully instrumented. Data analysis was performed to study the effect of several design parameters on axial stress in piles. An analysis of the pile-soil system was performed using the finite difference software LPILE. The maximum displacement of the bridge superstructure obtained from the FE model due to a maximum expected temperature change of $\pm 42^\circ\text{C}$ during the lifetime of the bridge was applied to the substructure model. The effect of bridge skew on the build-up of soil pressure behind the abutment was studied. A significant increase in the soil pressures and axial stresses behind the abutment at the obtuse side versus the acute was observed. The effect of the size of the galvanized steel sleeve on the induced axial stresses in piles was studied. We found that increasing the size of the steel sleeve increases their capacity to resist bending.

Keywords: Integral abutment, Soil-pile interaction, Laterally loaded piles, Full-scale testing, Finite element analysis

Introduction

Integral abutments are continuous bridges, where the deck is rigidly connected to the abutments and approach slabs. This rigid connection allows integral bridges to act as a single unit in resisting thermal and brake loads. The need for jointless bridges evolved from the desire to eliminate the use of expansion joints and bearings. The leak of deck drainage water contaminated with deicing chemicals has caused the deterioration of beam ends, pedestals, and piers. Moreover, expansion joints are expensive to buy, maintain, or replace. Bearings may grind to a halt due to lack of lubrication or progressive corrosion (Wasserman and Walker 1996). However, the impact of thermal loading on the abutment-pile system and the surrounding soil represents a crucial factor in the design of integral bridges and is considered the biggest obstacle in the analysis and design of such bridges. As such, the soil-structure interaction constitutes the focus of the research presented herein, in particular, the development of axial stresses in the piles supporting the

abutment as a result of thermal expansions and contractions of the bridge superstructure.

The daily and seasonal temperature changes, the changing temperature conductivity between the different components of the bridge superstructure, and the nonuniformity of the temperatures within the bridge deck in both the horizontal and vertical directions result in cyclic bridge expansions and contractions (Arsoy et al. 1999).

The behavior of pile-soil interaction has been studied using experimental and numerical analyses. The subgrade reaction approach provides the simplest solution for the pile-soil interaction problem. In this approach, the pile is treated as an elastic laterally loaded beam. The soil is idealized as a series of independent springs with constant stiffness, where the lateral load at one point does not affect the lateral load at other points along the depth of the pile (Reese and Matlock 1956; Broms 1964). The spring stiffness, or modulus of subgrade reaction, is defined as the ratio of the soil reaction per unit length of the pile as described in the following equation:

$$p = K_h y \quad (1)$$

* Correspondence: ykhodair@bradley.edu

¹Department of Civil Engineering and Construction, Bradley University, 1501 West Bradley Avenue, Peoria, IL 61625, USA

Full list of author information is available at the end of the article

where p is the soil resistance per unit length of the pile, K_i the modulus of subgrade reaction, and y the lateral deflection of the pile. However, a drawback of the method is its inability to account for the nonlinearity and continuity of soil.

The concept of a p - y curve was first introduced by McClland and Focht (1958). Brown and Shie (1990, 1991) developed three-dimensional (3D) finite element (FE) models to derive p - y curves. In these models, a simple elastic-plastic material model was used for the soil to study undrained static loading in clay soils. A plain strain finite element model that is symmetrical about the centerline of the bridge was developed by Arsoy et al. (1999). Linear stress-strain constitutive model was used to model the abutment. The approach fill and the foundation soil were modeled using hyperbolic material properties. The loads applied on the model represent the loads reflected from the superstructure and the abutment. Faraji et al. (2001) studied the effect of thermal loading on integral bridges using a three-dimensional FE model. The p - y method was used to model the nonlinear behavior of the soil behind the abutment and surrounding the piles. The soil pressure distribution on the abutment is typically nonlinear and varies with depth, amount, and mode of wall displacement. A small parametric study was conducted to study the effect of the level of soil compaction on the response of the pile-soil system. Thompson (1977) used a two-dimensional finite element model to obtain p - y curves for laterally loaded piles. The soil was modeled as an elastic-hyperbolic material. A one-dimensional finite element model was developed by Desai and Kuppusamy (1980). In their model, the soil was modeled using nonlinear springs and the pile as a beam column element. The soil was defined using the Ramberg-Osgood model. Faruque and Desai (1982) implemented both numeric and geometric nonlinearities in their three-dimensional finite element model. The Drucker-Prager plasticity theory was adopted to model the nonlinear behavior of the soil. Kumar (1992) investigated the behavior of laterally loaded single piles and pile groups using a three-dimensional nonlinear finite element modeling. Rajashree and Sitharam (2001) developed a nonlinear finite element model of batter piles under lateral loading. In their model, the nonlinear soil behavior was modeled using a hyperbolic relation for static load condition and modified hyperbolic relation, including degradation and gap for cyclic load condition. Olson et al. (2009) developed three-dimensional finite element analyses using SAP2000 to evaluate skew and maximum length of the integral bridges. The numerical analyses showed that acceptable bridge length and skew combinations that result in stresses below the yielding stress are affected by the grade of steel used for the piles and by the use of moment-reducing elements.

Other researchers have studied integral bridges using experimental analysis. Jorgensen (1983) instrumented an integral bridge for a period of 1 year. The analysis of the data proved that stresses at the top of the pile were sufficient to initiate a yield stress in the steel. Lawver et al. (2000) instrumented and monitored a bridge near Rochester, Minnesota for several years. It was found that the piles deform in double curvature, with the pile strains on the approach panel sides of the piles which indicates the beginning of yielding. Girton et al. (1991) instrumented two skewed bridges in IA, USA. The authors found that the stress in the piles may reach 60% to 75% of the yield stress, over the 1-year period.

The objectives of this research are to study (1) the maximum displacement that the Scotch Road integral abutment bridge can be subjected to due to thermal loading; (2) the effect of relevant design parameters which include the abutment temperature, displacement of the superstructure during thermal loading, abutment rotation, and soil pressure behind the abutment on the pile axial stresses; (3) the effect of bridge skew on the variation of soil pressure behind the abutment and axial stresses induced on the piles supporting the abutments; and (4) the effect of increasing the amount of sand surrounding the piles on its induced axial stresses. To that end, we (1) instrumented the abutment and piles during construction, (2) developed 3D FE model of the full bridge, a 2D finite difference (FD) method model using LPILE, (3) analyzed the effect of crucial design parameters on pile axial stress, and (4) studied the effect of the size of the galvanized steel sleeve on pile axial stress. Then, we draw our conclusion.

Bridge description

The Scotch Road I-95 integral bridge is located in the Ewing/Hopewell Township in NJ, USA. The bridge is composed of two spans of 45.5-m long continuous, integral abutment bridge as shown in Figure 1. The new bridge will accommodate two traffic lanes, one auxiliary lane, one shoulder, and one walkway in each direction with a total width of 32.91 m and an approximately 15° skew angle. The superstructure of the bridge consists of a composite section including the reinforced concrete bridge deck supported by ten high performance steel girders. An elevation view of the north integral abutment supported by the steel HP piles is shown in Figure 2.

The substructure is composed of reinforced concrete integral stub abutments (0.9 m in width and 2.88 m in depth) supported by 19 HP 360 × 152 steel piles embedded into the abutment walls to ensure full moment transfer as depicted in Figure 2. The relief slab is connected rigidly to the integral abutment from one side and supported by a sleeper slab from the other side. The soil behind the abutment and under the approach slab

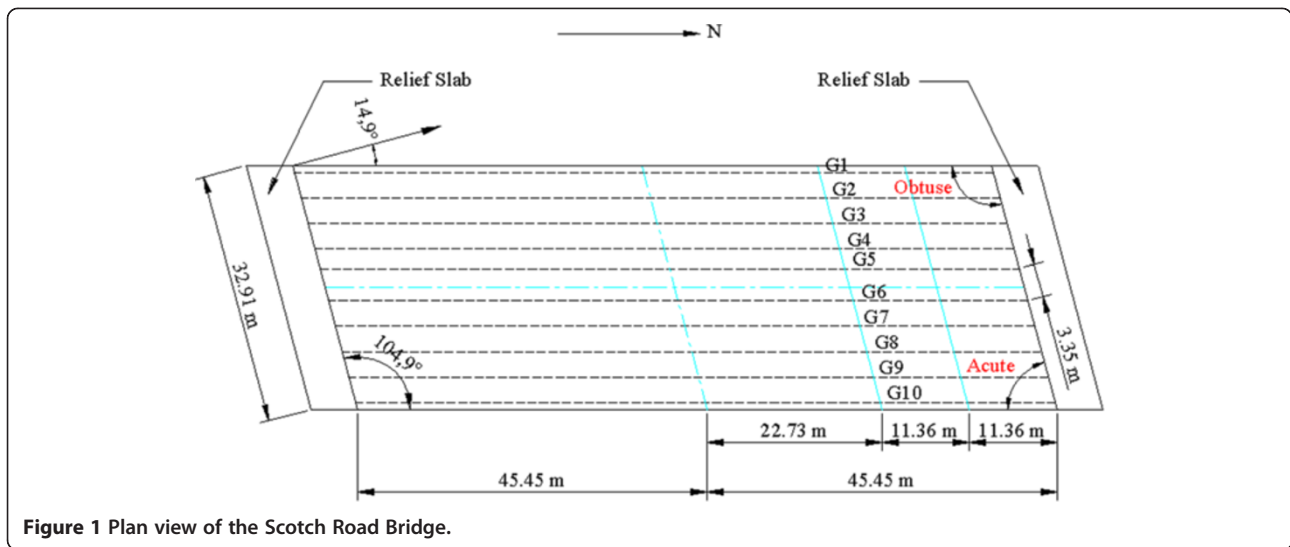


Figure 1 Plan view of the Scotch Road Bridge.

consists of well-compacted porous fill. The piles were first installed into pre-augured holes of 0.76 m in diameter. Then, the concrete was poured to cover up to 60% of the pile length, equivalent to 7.62 m of the total pile length. Next, a corrugated steel sleeve was inserted, supported by the concrete base, and extended to the top of the pile. The gap between the pile and the sleeve was filled with sand to facilitate the movement of the piles as subjected to lateral loads transferred from the superstructure. The piles were oriented such that bending would take place around their weak axes to increase the flexibility of the piles. Compacted crushed stone was used as a backfilling material between the piles, and the steel mesh was used to tie the components of the mechanically stabilized (MSE) wall. The MSE wall is a retaining structure surrounding the piles and the backfill soil between them. It consists of several panels

stacked on top of each other and tied laterally using soil-stabilizing steel meshes.

Methods

Experimental approach

The substructure of the Scotch Road I-95 integral abutment bridge was instrumented using six types of measuring devices: (1) 15 electrical resistant strain gages to measure strains along the depth of the piles, where each strain gage is composed of four resistances connected together to form a Wheatstone bridge circuit; (2) two tiltmeters to measure the rotations at the connection between the abutment and the second and fifth girders (G2 and G5); (3) two temperature sensors to measure the temperature of the abutment at the second and fifth girders (G2 and G5); (4) two round displacement transducers that were connected to the four strain gages to

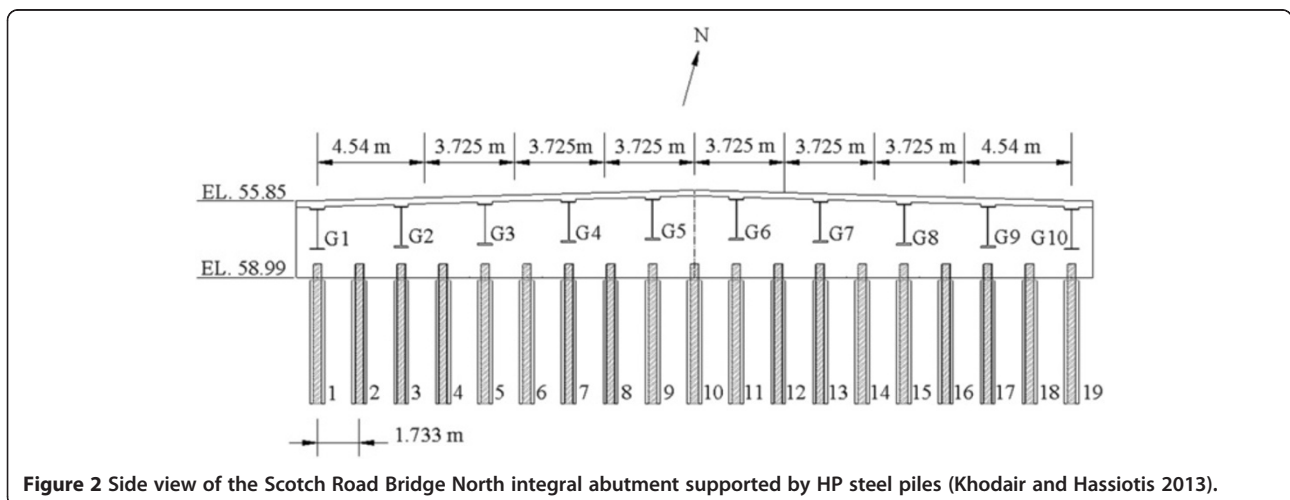


Figure 2 Side view of the Scotch Road Bridge North integral abutment supported by HP steel piles (Khodair and Hassiotis 2013).

measure the displacement at the east and west ends of the north relief slab; (5) eight thermocouples to measure the temperature variations in the bridge deck at the second and ninth girders (G2 and G9); and (6) 18 soil pressure cells to measure the horizontal soil pressure behind the abutment on the galvanized steel sleeves surrounding the piles (Khodair and Hassiotis 2013). The soil pressure cells were manufactured and calibrated in the laboratory before being installed on site. Figures 3 and 4 show the locations of the instrumented piles and north abutment.

Data acquisition was achieved using the CR 5000 measurement and control system manufactured by Campbell Scientific, Inc (UT, USA). The CR 5000 is a standalone system that was connected to a laptop computer. A serial link interface was used to connect the CR5000 system and the computer. A programming code was developed to control the flow of data. The data were gathered every 1 hour at the top of the hour.

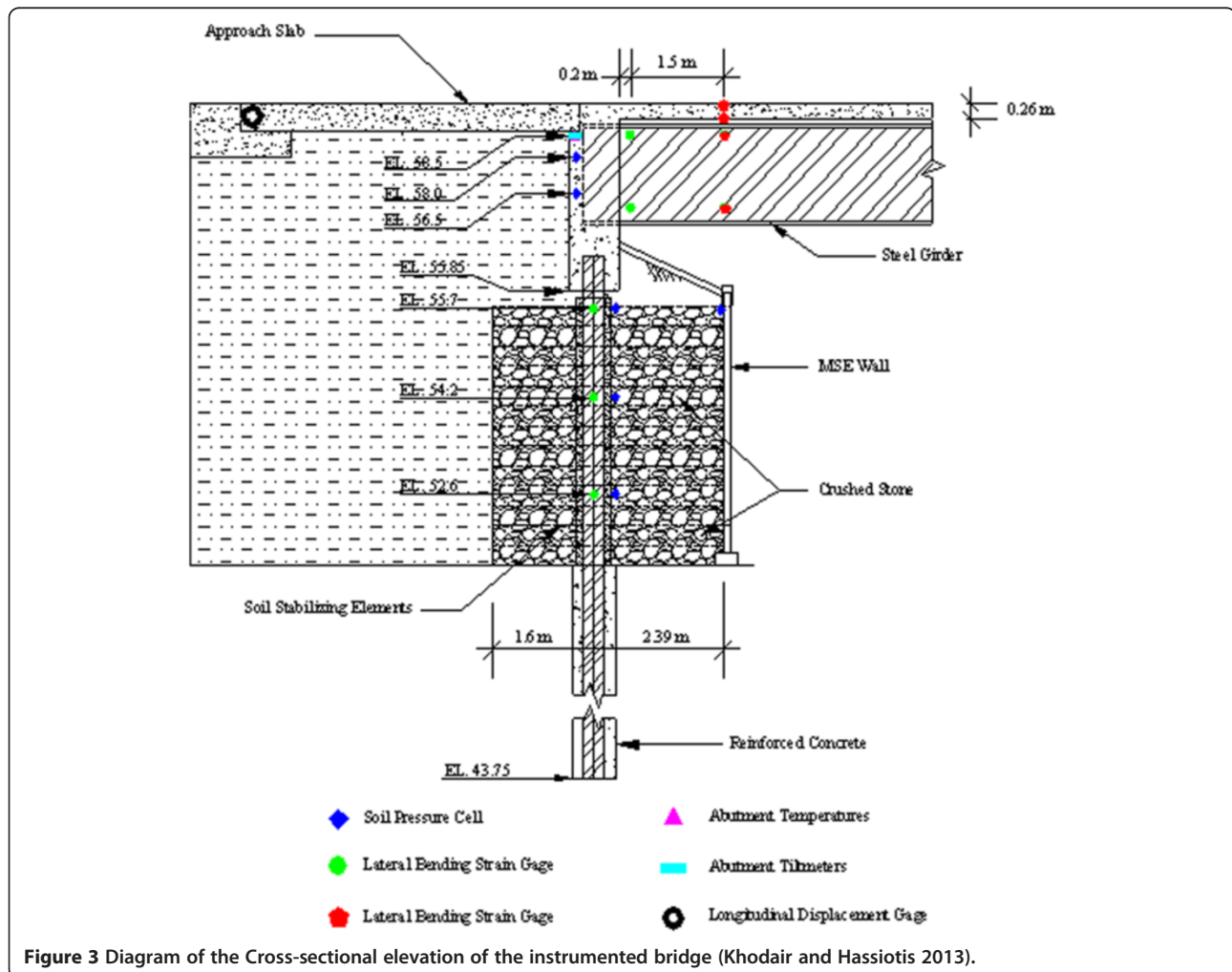
Results and discussion

Analysis of field data

The Scotch Road I-95 integral abutment bridge has been instrumented during two construction stages (I and II). The effect of some of the crucial design parameters such as abutment temperature, approach slab displacement, abutment rotation, soil pressure on axial stresses in piles, and the effect of bridge skew on soil pressure is discussed below.

Effect of abutment temperature on pile axial stress

The repetitive increase or decrease in temperatures causes expansion or contraction movements of the superstructure of the bridge during the passive and active pressure cycles. The relation between the axial stresses in piles #3, #6, and #9 and the abutment temperatures at G2 is described in Figure 5. As the abutment temperatures increase during March to August, the magnitude of the axial stresses increase with



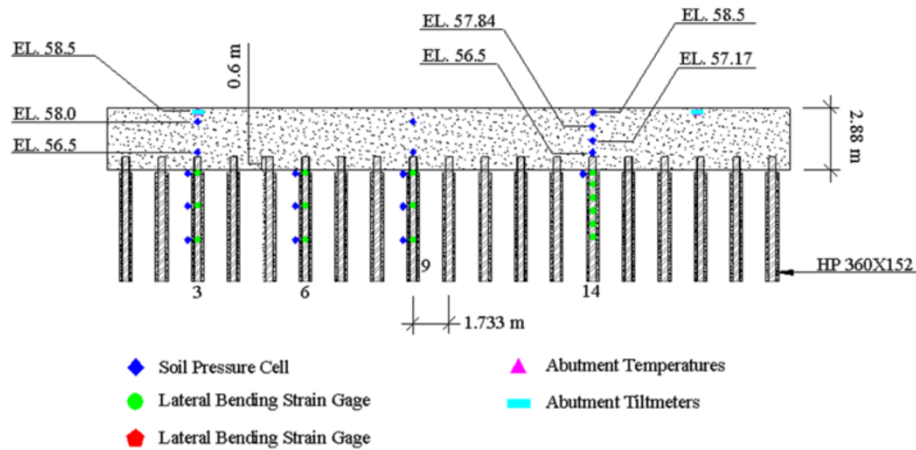


Figure 4 Diagram for the side view of the instrumented bridge (Khodair and Hassiotis 2013).

negative magnitudes during the passive pressure cycle. The negative magnitudes indicate tension stresses at the north face of the pile and compression at the south as shown in Figure 6. To the contrary, as the abutment temperatures decrease during September to February, the magnitude of the axial stresses also increases, with positive magnitudes indicating compression stresses at the north and tension at the south faces, respectively.

Effect of approach slab displacement on piles axial stress

The approach slabs are floored with two sheets of polyethylene acting as bond breakers to alleviate or even eliminate the friction between the approach slab and the soil

underneath it. Therefore, the displacements at the end of the approach slabs are approximately the same as those at the top of the abutments. The displacement rings were configured such that negative displacement magnitudes correspond to an increase in the abutment temperatures and an overall expansion of the bridge superstructure during the passive pressure cycle. However, the positive displacement magnitudes correspond to a decrease in abutment temperatures and an overall contraction of the bridge superstructure during the active pressure cycle. Figure 7 shows that as the displacements increase with negative magnitudes, the axial stresses increase with negative magnitudes, indicating tension in the north face of the pile and

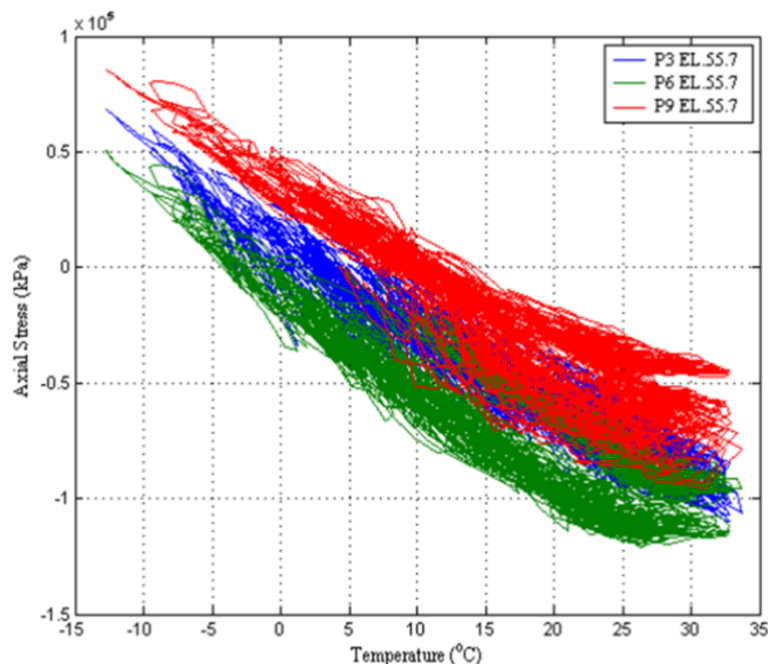


Figure 5 Effect of abutment temperature variations on axial stresses in piles #3, #6, and #9.

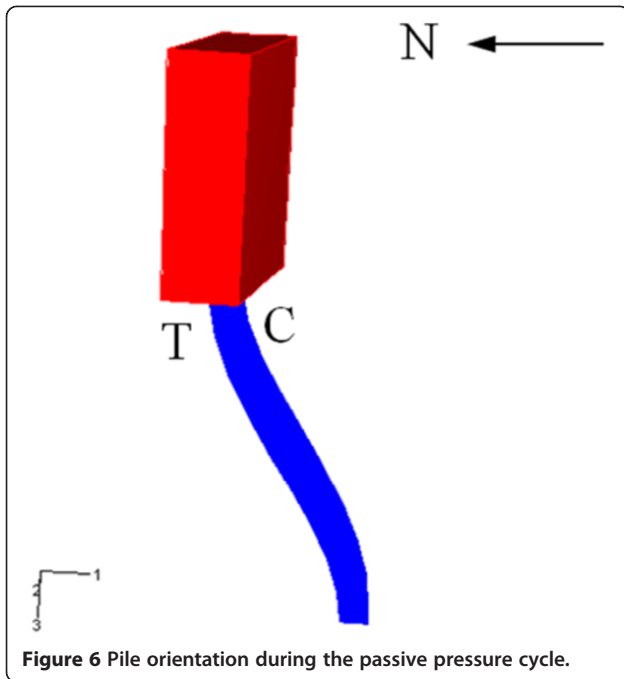


Figure 6 Pile orientation during the passive pressure cycle.

compression on the south as shown in Figure 6. The same trend is observed for the increase in the positive displacements, which are also associated with a corresponding increase in the positive bending stresses.

Effect of abutment rotation on pile axial stress

The tiltmeters used to measure the rotations of the abutment were configured such that rotations towards the

retained soil during the passive pressure cycle correspond to the rotations of negative magnitudes, and rotations away from the retained soil during the active pressure cycle correspond to positive magnitudes. Figure 8 shows that as the magnitudes of the measured rotations of the abutment increase with negative magnitudes, the magnitudes of the axial stresses increase with negative magnitudes accordingly. This indicates that the displacements at the end of the approach slabs and rotations at the top of the abutment have the same effect on the axial stresses of the piles, which are increasing the stresses with negative magnitudes during the passive pressure cycles and increasing them with positive magnitudes during the active pressure cycles.

Effect of soil pressure on pile axial stress

As the soil pressures in piles #3, #6, and #9 behind the abutment increase in magnitude during the period from March to August (passive pressure cycle), the bending stresses increase with negative magnitudes. However, as the magnitudes of the soil pressures drop from September to February (active pressure cycle), the bending stresses increase with positive magnitudes as shown in Figure 9.

Effect of bridge skew

The Scotch Road I-95 integral abutment bridge has a 15° skew angle as mentioned before. Figure 10 shows the discrepancy in the magnitudes of the soil pressure at piles #3, #9, and #14. Although, piles #3, #6, and #9 were constructed during stage I of the project, and pile #14 in

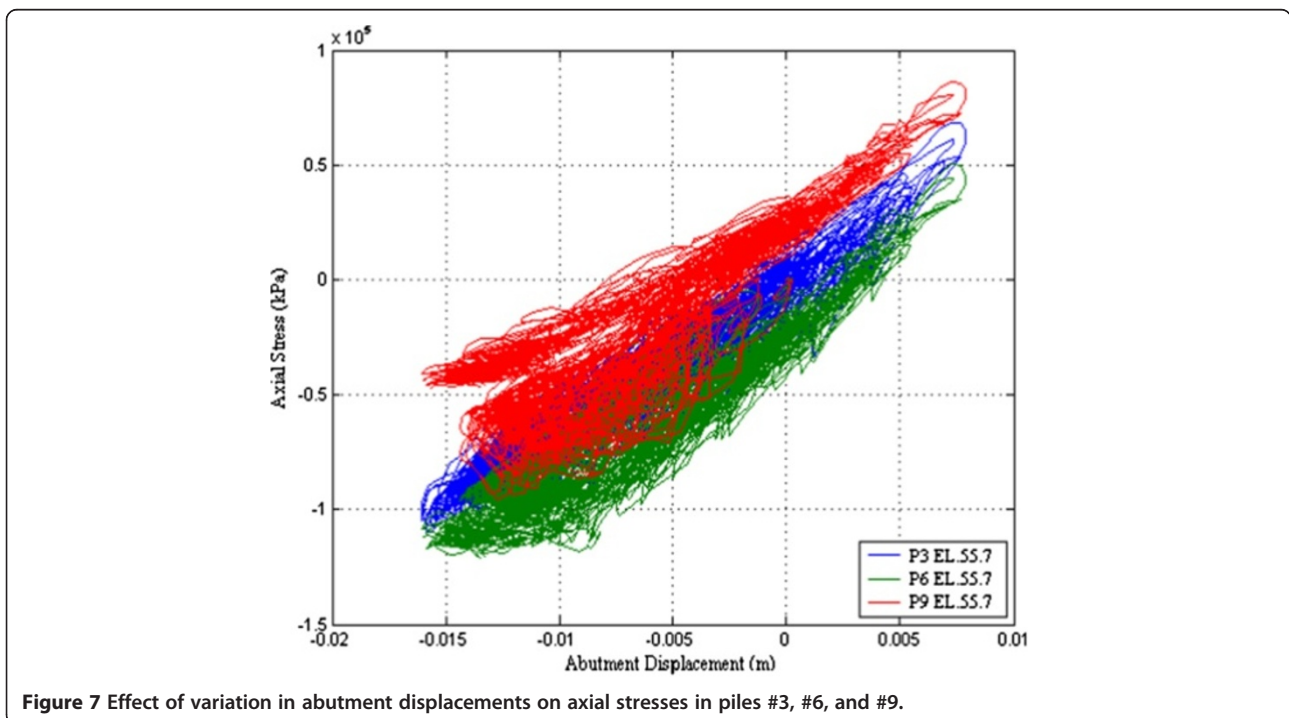


Figure 7 Effect of variation in abutment displacements on axial stresses in piles #3, #6, and #9.

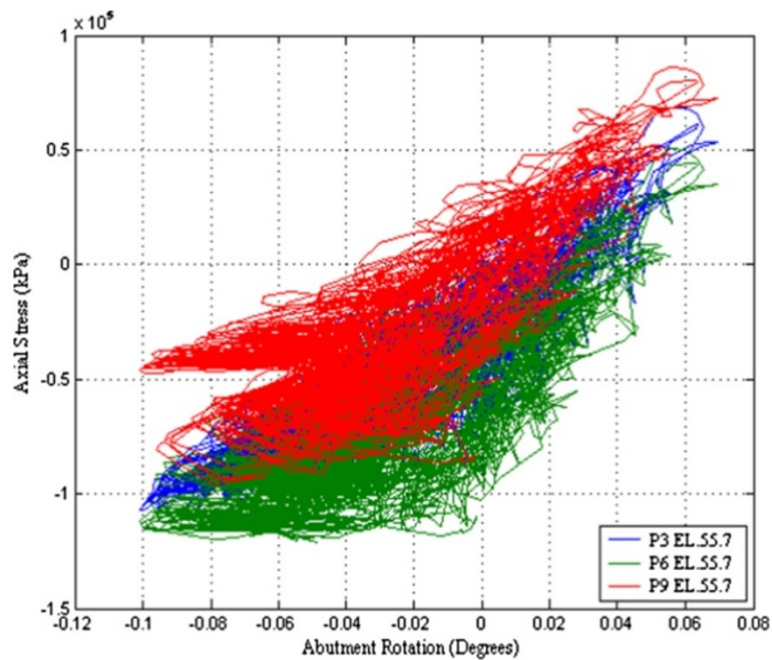


Figure 8 Effect of variation in abutment rotations on axial stresses in piles #3, #6, and #9.

stage II, comparing the soil pressures that accumulated on the abutment for the first few months at each location, it shows that a large difference in magnitudes that cannot be accounted for by the pressure built up due to cyclic loading alone. This difference is primarily attributed to the position of the pressure cells with respect

to the skew angle of the bridge. The soil pressure cells in piles #3, #6, and #9 are positioned towards the obtuse side of the bridge, where the level of soil compaction is lower than that of the acute. The reduced level of confinement of the retained soil behind the abutment at the obtuse side of the bridge allows for greater lateral

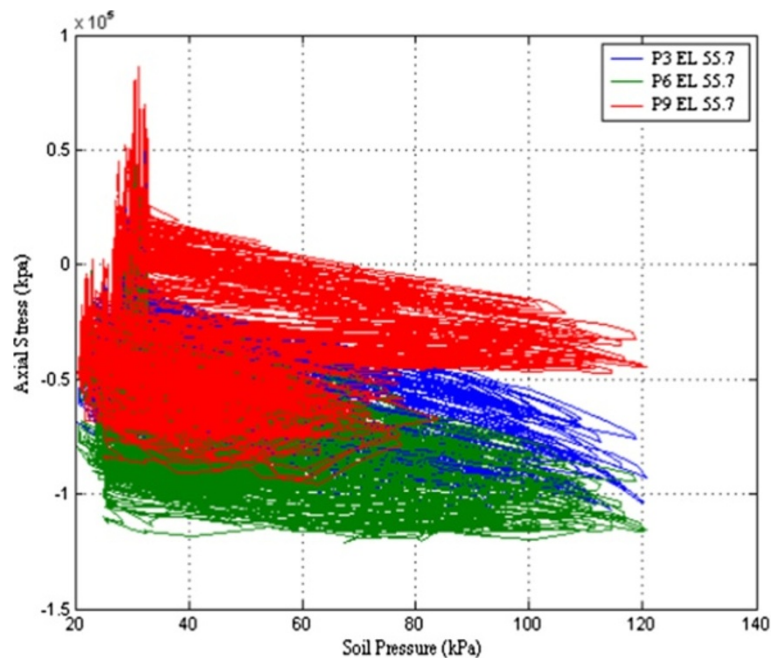


Figure 9 Effect of variation in soil pressures behind abutment on axial stresses in piles #3, #6, and #9.

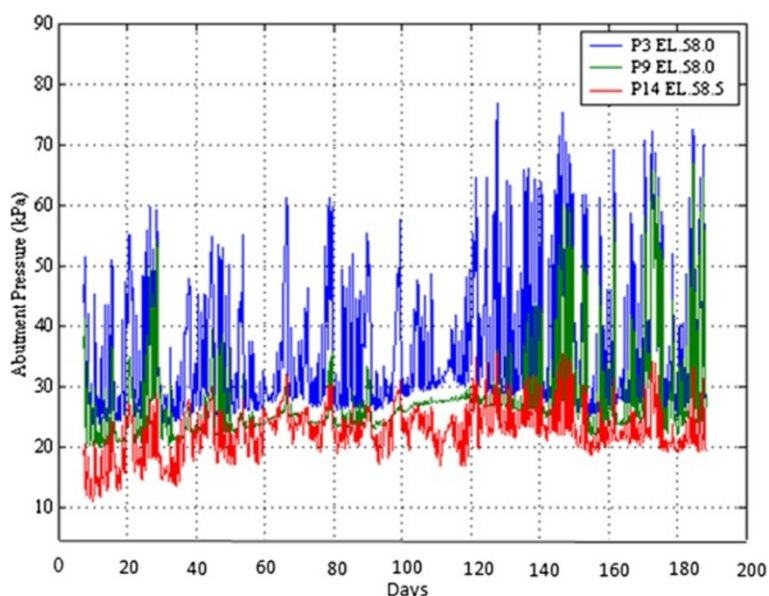


Figure 10 Distribution of abutment soil pressure in piles #3, #9, and #14 with time.

movement of the abutment, and thus higher soil pressure than that accumulated at the acute side. This resulted in higher axial stresses in piles #3, #6, and #9 versus those calculated at pile #14.

Finite element models

Two 3D finite element models were developed to study the effect of thermal loading on the superstructure and substructure of the Scotch Road integral abutment bridge. The FE models were developed using ABAQUS/Cae (ABAQUS Inc., RI, USA), a computer package with capabilities to address problems with soil-structure interaction.

Full bridge model

The geometry was modeled according to the exact dimensions of the superstructure and substructure of the Scotch Road integral abutment bridge, as shown in

Figure 11. Three types of elements were used in the full bridge model: (1) the four-nodded, shell elements were used to model the bridge deck, (2) three-nodded beam elements were used to model the I-shaped steel girders, and (3) two-nodded beam elements were used to model the reinforced concrete abutment and piles. The soil behind the abutments and under the approach slabs was modeled using Spring1 elements, which connect from the defined node to the ground. The reinforced concrete material definition for the bridge deck was assumed to be elastic-plastic. The modulus of elasticity for the concrete was considered to be 2.86×10^7 kN/m². Grade 70 steel I-beams were used to model the steel beams with a modulus of elasticity of 2.0×10^8 . An elastic-perfectly plastic material modeling was adopted for the steel beams. The modulus of elasticity of the steel piles was assumed to be 2.0×10^8 kN/m², and their yielding stress to be 344,750 kN/m².

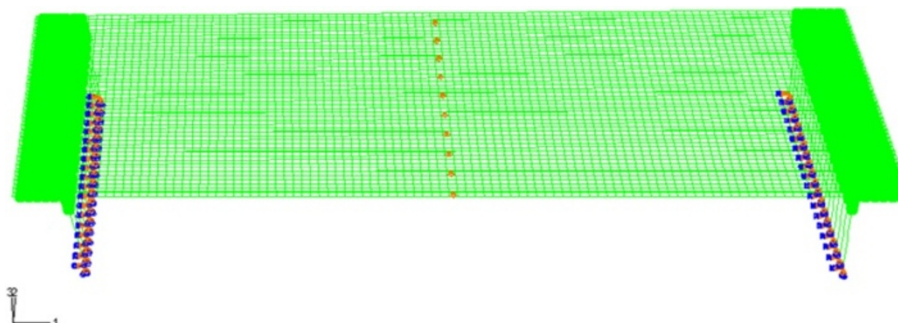


Figure 11 Boundary conditions for full bridge model.

Table 1 Modulus of subgrade reaction for soils behind abutments and under approach slabs

Structure type	Tributary area (m ²)		Modulus of subgrade reaction (kN/m)	
	Interior	Exterior	Interior	Exterior
Abutments	0.84395	0.421975	51,480.95	25,740.48
Approach slabs	0.67	0.335	40,870	20,435

The spring elements used to model the soil were presumed to be linear springs with constant modulus of subgrade reaction. A value of 61,000 kPa/m was used to represent the modulus of subgrade reaction in the model for the soil behind the abutment and below the approach slabs (Bowels 1996). Each interior spring has a tributary area, defined as the centerline-to-centerline distance between each other node, along the longitudinal and transverse directions. However, exterior springs carry half the tributary area defined for the interior. The modulus of subgrade reaction for linear springs is estimated according to the following equation:

$$K_s(\text{kN/m}) = 61,000 \text{ kPa/m} * A_{\text{tributary}} \quad (4.1)$$

Table 1 shows the values of the modulus of subgrade reaction used in the full bridge model for exterior and interior springs for the soil behind the abutments and under the approach slabs. Three boundary conditions were imposed on this model, corresponding to modeling the bridge as a frame-like structure. The embedment of the piles below a depth of 5.182 m into the plain concrete was modeled using a fixed-type connection. A roller support was imposed at the middle of the bridge corresponding to the support provided by the piers for the bridge superstructure, as shown in Figure 11. The composite section between the steel girders and the bridge deck was

modeled using multipoint constraints (MPC). MPC-type beam provides a rigid beam between two nodes to constrain the displacement and rotation at the first node to the displacement and rotation at the second node, corresponding to the presence of a rigid beam between the two nodes (Hibbitt, Karlsson & Sorensen, Inc 2009). The temperature variations between the top and bottom flanges of the second girder (G2), along with those between the top and bottom of the bridge deck were applied to the full bridge model for the sake of comparison. However, the field data collection is not sufficient to monitor the thermal behavior of the bridge during the changes in temperature between the different seasons over a long period of time and to determine the movement of the bridge during its predicted lifetime. Therefore, it was necessary to predict the deflections that the bridge undergoes, as subjected to extensive thermal expansions or contractions. A temperature change of $\pm 42^\circ\text{C}$ (AASHTO LRFD 2012) was applied to the bridge deck, assuming an isotropic material behavior. Figure 12 shows the deformed shape of the bridge expansion due to thermal loading, where the maximum displacement of the bridge superstructure was found to be approximately 0.02 m.

Soil-pile interaction FE model

The 3D soil-pile interaction model (Khodair and Hassiotis 2013) was developed to fully simulate the actual behavior

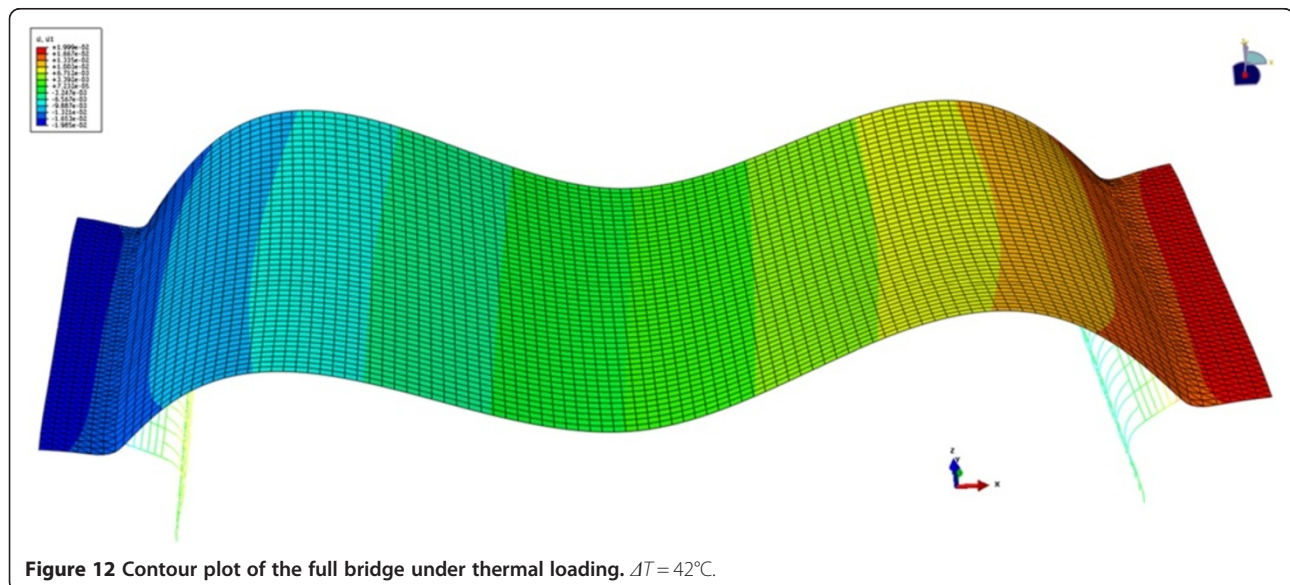


Figure 12 Contour plot of the full bridge under thermal loading. $\Delta T = 42^\circ\text{C}$.

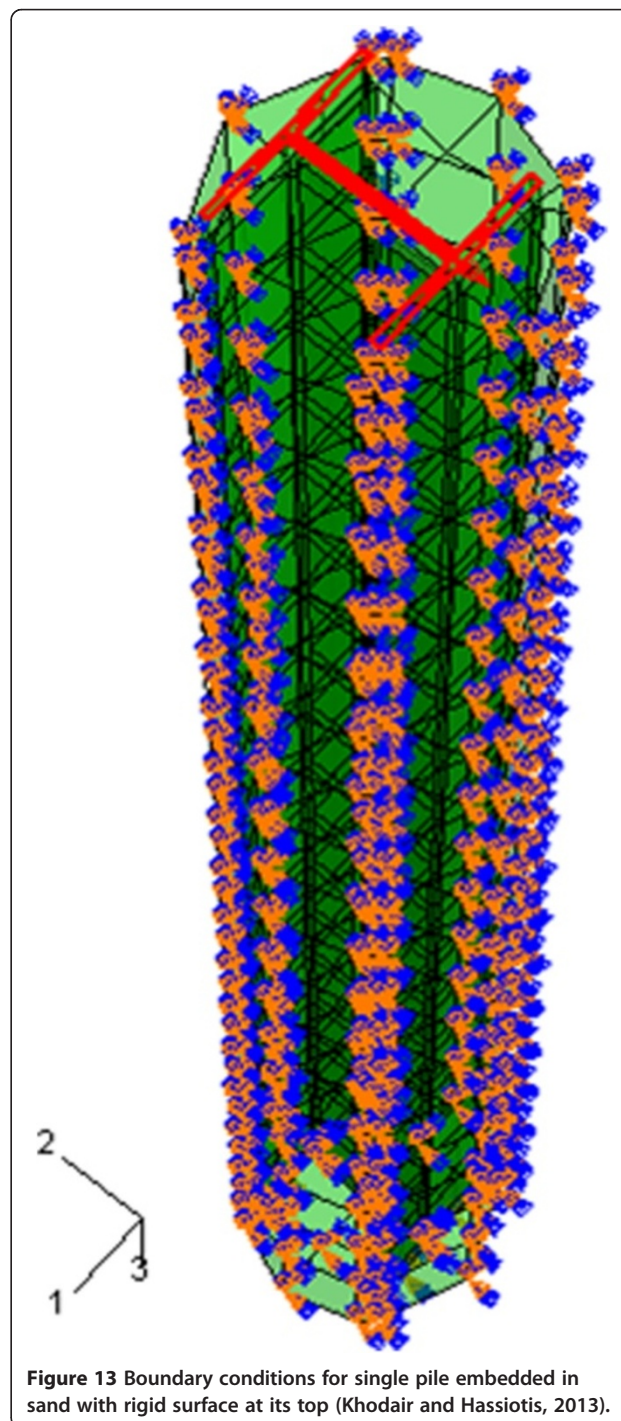
of the piles and their interaction with the soil. In this model, the pile and soil were modeled using eight-nodded solid continuum elements. Three boundary conditions were imposed in the FE model: (1) fixed conditions at the bottom of the pile at a depth of 5.182 from the top of the piles to model the embedment of the piles in plain concrete, (2) restraining all degrees of freedom associated with the exterior surface of the sand surrounding the piles to model the confinement of the galvanized steel sleeves by crushed stone backfill, and (3) guided fixation at the top of the pile modeled by tying the nodes at the top surface of the pile to a defined reference point located in the centroid of the cross-section of the pile at its top to simulate the embedment of the piles into the abutments, as shown in Figure 13.

The steel piles were modeled using an elastic-perfectly plastic model. The soil was modeled using a strain hardening model implementing Mohr-Coulomb failure criterion. The soil-pile interaction was simulated by adopting tangential and normal contact behavior in the model. Master and slave surfaces were defined in the model such that the exterior surface of the pile was used to model the master surface, and the interior surface of the sand was used for the slave surface. A friction coefficient of 0.44 (Venkatramiah 2006) and an angle of internal friction ϕ of 30° to 38° (Bowels 1996) were used to define the tangential contact between the two surfaces and the variation in the density (loose to dense) of sand surrounding the pile. A variation in Young's modulus for the sand between 27,000 and 69,000 kN/m² was adopted along the depth of the pile in the FE model. The steel piles modulus of elasticity was assumed to be 2×10^8 kN/m², and their yielding stress to be 344,750 kN/m². The computed dead and live loads of 692 KN were applied as a concentrated load to the reference point of the rigid body along the depth of the pile defined as global (three direction). The self-weight was incorporated into the model using a gravity step, where the density of the materials and gravity acceleration are specified. The dead and live loads were applied prior to the application of the lateral loading to maintain their effect in full during the lateral deflection step.

Parametric study

A limited parametric study was conducted to study the effect of the size of the galvanized steel sleeve and, hence, the amount of sand surrounding the pile on its induced axial stresses (Khodair and Hassiotis 2005). The 3D finite element model of soil-pile interaction (Khodair and Hassiotis 2013) was used to study the effect of the size of the galvanized steel sleeve and, hence, the amount of sand surrounding the pile on its induced axial stresses. The lateral loading that was obtained from the 3D finite element model of the full bridge (0.02 m) which

corresponds to the maximum temperature increase/decrease of $\pm 42^\circ\text{C}$ that the bridge could be subjected to during its lifetime was applied to the soil-pile interaction FE model while varying the diameter of the steel sleeve surrounding the pile. The diameter of the steel sleeve was assumed to vary from 0.6 to 2.5 m. The FE model shows that as the diameter of the steel sleeve increases, which indicates an increase in the amount of sand



surrounding the piles, the magnitudes of the axial stresses decrease accordingly; hence, the gap in the magnitudes of the axial stresses calculated based on the finite element model and those obtained from LPILE (Ensoft 2012) reduced significantly as shown in Figure 14. The reason for the discrepancy in the magnitudes of the axial stresses induced in the piles between LPILE and the soil-pile interaction FE model is attributed to the fact that LPILE analysis is based on a single pile embedded in an extended single layer of sand.

Conclusions

The analysis of the soil-structure interaction in integral abutment bridges under thermal loading has always been a concern. In this paper, experimental and numerical analyses have been conducted to study the effect of thermal loading on the superstructure and substructure of the Scotch Road I-95 integral abutment bridge. The bridge superstructure and substructure were fully instrumented using strain gages, tiltmeters, temperature sensors, round displacement transducers, and thermocouples. The field data were gathered using the CR 5,000 measurement and control system manufactured by Campbell Scientific, Inc. The data were collected every 1 hour at the top of the hour. The data analysis showed excellent correlation between the abutment temperature, approach slab displacement, abutment rotation, soil pressure and the piles axial stress, which indicates that the strain gages are working properly. The data analysis showed that as the temperature increases, the

displacements at the end of the approach slab and the rotations at the abutment increase with negative magnitudes, resulting in an overall expansion of the bridge during the passive pressure cycles. This results in an increase in axial stresses with negative magnitudes, indicating tension in the north face of the pile and compression on the south. However, as the temperature decreases, the displacements at the end of the approach slab and the rotations at the abutment increase with positive magnitudes, resulting in an overall contraction of the bridge during the active pressure cycles. This results in an increase in the positive axial stresses, indicating compression in the north face of the pile and tension on the south. The effect of bridge skew on the build-up of soil pressures and the axial stresses in the piles was studied. The data showed that there is an increase in the soil pressure towards the obtuse side of the bridge versus the acute because the reduced level of confinement of the retained soil behind the abutment at the obtuse side results in greater flexibility in the abutment movement, hence higher soil pressures. This larger movement of the abutment at the obtuse side has resulted in higher axial stresses in piles #3, #6, and #9 versus those calculated in pile #14.

A 3D FE model was developed of the Scotch Road I-95 integral abutment bridge (full bridge model) using ABAQUS/Cae. The full bridge FE model consisted of shell elements for the bridge deck, approach slabs, beam elements for the steel girders, abutment, and piles. Spring elements were used to model the soil. The

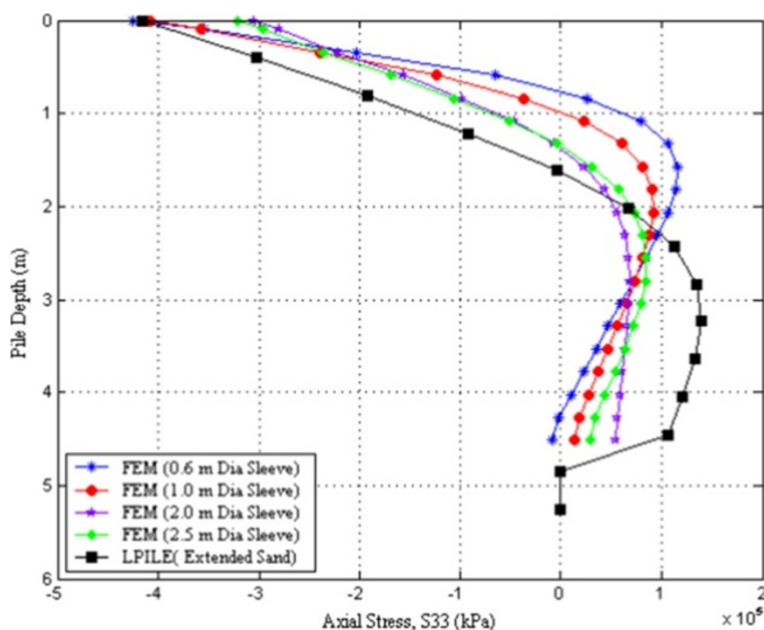


Figure 14 Comparison of the axial stresses. These stresses were obtained from FE and FD solutions at different sand sleeve diameters due to thermal loading. $\delta = 0.02$ m.

composite action between the steel girders and the bridge deck was modeled using MPCs. A temperature change of $\pm 42^{\circ}\text{C}$ was applied to the bridge deck to determine the maximum displacement that the bridge could be subjected to over its predicted lifetime. The results from the model showed that the maximum displacement of the bridge superstructure is 0.02 m. The 3D soil-pile interaction model consisted of solid continuum elements for both the piles and soil. The contact behavior between the piles and the soil was defined using tangential and normal algorithms in ABAQUS/Cae. Mohr-Coulomb failure criterion was used to model the nonlinear response of the soil. A limited parametric study was conducted to study the effect of the size of the galvanized steel sleeve on the induced axial stresses in piles. The soil-pile interaction model was compared to FD solutions for a single pile embedded in sand under a displacement of 0.02 m obtained from the finite element model of the full bridge while varying the diameter of the steel sleeve surrounding the pile. The results from FE and FD analyses showed that the discrepancy in the magnitudes of the axial stresses and displacements from both analyses was substantially reduced with the increase in the size of the steel sleeve surrounding the pile approaching an extended single layer of sand. This indicates that increasing the size of the steel sleeve and the amount of sand surrounding the piles reduces the induced axial stresses in the piles, thus increases their capacity to resist bending.

Competing interest

The authors declare that they have no competing interests.

Authors' contributions

YK developed the three-dimensional finite element models, analyzed the results, and drafted the manuscript. YK conducted the literature review. Both YK and SH participated in the instrumentation and the analysis of the data collected from the field. Both authors read and approved the final manuscript.

Authors' information

YK holds the position of an Assistant Professor in the Department of Civil Engineering and Construction at Bradley University. SH holds the position of an Associate Professor at the Department of Civil, Environmental, and Ocean Engineering at Stevens Institute of Technology.

Acknowledgments

This work was supported by the New Jersey Department of Transportation (NJDOT).

Author details

¹Department of Civil Engineering and Construction, Bradley University, 1501 West Bradley Avenue, Peoria, IL 61625, USA. ²Department of Civil, Environmental and Ocean Engineering, Stevens Institute of Technology, Castle Point on Hudson, Hoboken, NJ 07054, USA.

Received: 5 September 2012 Accepted: 8 April 2013

Published: 1 May 2013

References

AASHTO LRFD (2012) Bridge design specifications, 6th edn. American Association of State Highway and Transportation Officials, Washington DC

- Arsoy S, Barker RM, Duncan JM (1999) The behavior of integral abutment bridges (VTRC 00-CR3). Virginia Transportation Research Council, Charlottesville, VA
- Bowels J (1996) Foundation analysis and design, 5th edn. McGraw-Hill, New York
- Broms B (1964) Lateral resistance of piles in cohesionless soils. *J Soil Mech Found Div*, (ASCE) 90(3):136–156
- Brown DA, Shie C-F (1990) Three dimensional finite element model of laterally loaded piles. *Comput Geotech* 10(1):59–79
- Brown DA, Shie C-F (1991) Some numerical experiments with a three dimensional finite element model of a laterally loaded pile. *Comput Geotech* 12(2):149–162
- Desai CS, Kuppusamy T (1980) Application of a numerical procedure for laterally loaded structures. In: Numerical methods in offshore piling. Institution of Civil Engineers (ICE), London, pp 93–99
- Ensoft (2012) LPILE Plus 6.0 geotechnical analysis program. <http://www.ensoftinc.com>. Accessed 05 Dec 2012
- Faraji S, Ting J, Crovo D, Ernst H (2001) Nonlinear analysis of integral bridges: finite-element model. *J Geotech Geoenviron Eng*, (ASCE) 27(5):454–461
- Faruque MO, Desai CS (1982) 3-D material and geometric non-linear analysis of piles. Paper presented at the second international conference on numerical methods for offshore piling, Austin, TX, 29–30 April 1982
- Girton DD, Hawkinson TR, Greimann LF (1991) Validation of design recommendations for integral abutment piles. *J Struct Eng* 117:2117–2134
- Hibbitt, Karlsson & Sorensen, Inc (2009) ABAQUS/Standard 6.9.1 User Manuals. ABAQUS, Inc, RI, USA
- Jorgensen JL (1983) Behavior of abutment piles in an integral abutment in response to bridge movements. *Transport Res Board* 903:72–79
- Khodair Y, Hassiotis S (2005) Analysis of soil-pile interaction in integral abutment. *Comput Geotech* 32:201–209
- Khodair Y, Hassiotis S (2013) Rigidity of abutments in integral abutment bridges. *Struct Infrastruct Eng* 9(2):156–160
- Kumar S (1992) Three-dimensional non-linear finite element analysis of laterally loaded piles in clay, Dissertation, Edinburgh University
- Lawler A, French C, Shield CK (2000) Field performance of integral abutment bridge. *Transport Res Rec* 1740:108–117
- McCelland B, Focht JA (1958) Soil modulus for laterally loaded piles. *Trans Am Soc Civil Eng* (ASCE) 123:1049–1063
- Olson S, Long J, Hansen J, Renekis D, LaFave J (2009) Modification of IDOT integral abutment design limitations and details. Final Report, FHWA-ICT-09-054. Center of Transportation, Illinois
- Rajashree SS, Sitharam TG (2001) Nonlinear finite-element modeling of batter piles under lateral load. *J Geotechn Geoenviron Eng* 127(7):604–612
- Reese LC, Matlock H (1956) Non-dimensional solutions for laterally loaded piles with soil modulus assumed proportional to depth. In: University of Texas (ed) Proceedings of the 8th Texas conference on soil mechanics and foundation engineering, Sp. Pub. 29. Bureau of Engineering Research, University of Texas, Austin
- Thompson GR (1977) Application of finite element method to the development of p - y curves for saturated clays. Thesis, University of Texas, Austin, Texas
- Venkatramiah C (2006) Geotechnical engineering, 3rd edn. New Age International, New Delhi
- Wasserman EP, Walker JH (1996) Integral abutments for steel bridges. Highway structures design handbook, vol. II, chap. 5. American Iron and Steel Institute (AISI), Chicago, IL

doi:10.1186/2008-6695-5-14

Cite this article as: Khodair and Hassiotis: Numerical and experimental analyses of an integral bridge. *International Journal of Advanced Structural Engineering* 2013 5:14.